Cortactin deficiency is associated with reduced neutrophil recruitment but increased vascular permeability in vivo

Michael Schnoor,[1] Frank P.L. Lai,[2] Alexander Zarbock,[1,4] Ruth Kläver,[1] Christian Polaschegg,[1] Dörte Schulte,[1] Herbert A. Weich,[3] J. Margit Oelkers,[2,5] Klemens Rottner,[2,5] and Dietmar Vestweber[1]

[1]Max Planck Institute for Molecular Biomedicine, D 48149 Münster, Germany
[2]Cytoskeleton Dynamics Group and [3]Department of Gene Regulation and Differentiation, Helmholtz Centre for Infection Research, D 38124 Braunschweig, Germany
[4]Department of Anesthesiology and Critical Care Medicine, University of Münster, D 48149 Münster, Germany
[5]Institute of Genetics, University of Bonn, D 53117 Bonn, Germany

Neutrophil extravasation and the regulation of vascular permeability require dynamic actin rearrangements in the endothelium. In this study, we analyzed in vivo whether these processes require the function of the actin nucleation–promoting factor cortactin. Basal vascular permeability for high molecular weight substances was enhanced in cortactin-deficient mice. Despite this leakiness, neutrophil extravasation in the tumor necrosis factor–stimulated cremaster was inhibited by the loss of cortactin. The permeability defect was caused by reduced levels of activated Rap1 (Ras-related protein 1) in endothelial cells and could be rescued by activating Rap1 via the guanosine triphosphatase (GTPase) exchange factor EPAC (exchange protein directly activated by cAMP). The defect in neutrophil extravasation was caused by enhanced rolling velocity and reduced adhesion in postcapillary venules. Impaired rolling interactions were linked to contributions of β_2-integrin ligands, and firm adhesion was compromised by reduced ICAM-1 (intercellular adhesion molecule 1) clustering around neutrophils. A signaling process known to be critical for the formation of ICAM-1–enriched contact areas and for transendothelial migration, the ICAM-1–mediated activation of the GTPase RhoG was blocked in cortactin-deficient endothelial cells. Our results represent the first physiological evidence that cortactin is crucial for orchestrating the molecular events leading to proper endothelial barrier function and leukocyte recruitment in vivo.

CORRESPONDENCE
Dietmar Vestweber:
vestweb@mpi-muenster.mpg.de

Abbreviations used: CA, constitutively active; EPAC, exchange protein directly activated by cAMP; ES, embryonic stem; ESAM, endothelial cell–selective adhesion molecule; F-actin, filamentous actin; HUVEC, human umbilical vein endothelial cell; MLEC, murine lung endothelial cell; S1P, sphingosine-1-phosphate; siRNA, small interfering RNA; VE-cadherin, vascular endothelial cadherin; WASP, Wiskott-Aldrich syndrome protein.

Neutrophil extravasation is a central process of the immune system that enables neutrophils to survey the body and to reach sites of infection. Inflammatory signals lead to the expression of endothelial surface receptors such as E- and P-selectin that mediate capturing and rolling of neutrophils on the vessel wall. β_2-Integrins on neutrophils further slow down rolling and, triggered by chemokines, mediate neutrophil arrest followed by crawling and eventually diapedesis through the blood vessel wall (Ley et al., 2007; Schnoor and Parkos, 2008). These processes require the coordinated function of adhesion receptors, the cytoskeleton, and signaling molecules (Vestweber, 2007). During these processes, vascular permeability is usually increased, which may cause complications such as edema formation or sepsis if not properly controlled (Kumar et al., 2009).

Inflammatory stimuli that trigger leukocyte adhesion and transmigration also cause cytoskeletal rearrangements allowing for the morphological changes required for the opening of endothelial cell contacts and for the accommodation of leukocytes moving through these openings (Alcaide et al., 2009; van Buul and Hordijk, 2009). Especially in the cellular cortical regions, actin filaments are in a highly dynamic

F.P.L. Lai's present address is Institute of Medical Biology, Singapore 138648.

state that is nevertheless tightly regulated to facilitate sophisticated processes such as leukocyte adhesion and transmigration (Revenu et al., 2004). Adhesion of leukocytes to the endothelium is accompanied by the formation of endothelial adhesive structures that support firm adhesion and arrest of leukocytes and are enriched in the integrin ligand ICAM-1 (intercellular adhesion molecule-1) and filamentous actin (F-actin; Barreiro et al., 2002; Carman et al., 2003).

Cortactin is an actin-binding protein that promotes actin assembly (Ammer and Weed, 2008). Cortactin is ubiquitously expressed except for leukocytes that instead express the cortactin-related protein HS1 (hematopoietic cell–specific Lyn substrate 1; Kitamura et al., 1989; Burkhardt et al., 2008). Cortactin has a multidomain structure consisting of binding regions for the Arp2/3 (actin-related protein 2/3) complex and F-actin. These domains are followed by a proline-rich region containing several serine/threonine/tyrosine residues that are targets for different kinases and an SH3 (Src homology 3) domain at the C terminus through which cortactin can bind to a plethora of different proteins (Cosen-Binker and Kapus, 2006). Cortactin and HS1 were previously observed to increase Arp2/3 complex–dependent actin assembly in vitro, although the potency of Arp2/3 complex activation is below that of canonical, so-called type I Arp2/3 complex activators such as Wiskott-Aldrich syndrome protein (WASP) or WAVE (Uruno et al., 2003; Goley and Welch, 2006). Cortactin can also collaborate with the type I Arp2/3 complex activator N-WASP (neural WASP; Weaver et al., 2002), both of which were concluded to promote Arp2/3-dependent actin remodeling events such as cell migration (Kowalski et al., 2005). However, interpretation of these results is complicated by an increase rather than decrease in cell migration rates observed in N-WASP–defective cells (Misra et al., 2007) and by the recently determined less direct role that cortactin plays in this process. More specifically, cortactin is not required for the activation of Arp2/3 complex in lamellipodia or at sites of endocytosis, but instead appears to modulate the signaling pathways driving their formation (Lai et al., 2009). Consistent with this, HS1 is also dispensable for spreading and lamellipodia formation in platelets (Thomas et al., 2007). Clearly, the precise function of cortactin and HS1 in Arp2/3-dependent actin remodeling in vivo appears elusive to date.

In vitro studies of endothelial cells have provided some evidence for possible functions of cortactin in endothelial cells. Cross-linking of ICAM-1 was reported to stimulate tyrosine phosphorylation of cortactin (Durieu-Trautmann et al., 1994; Adamson et al., 1999) and enabled coprecipitation of cortactin with ICAM-1 (Tilghman and Hoover, 2002). Silencing of cortactin by small interfering RNA (siRNA) was found to inhibit transmigration of neutrophils through endothelial cell monolayers, but although this was accompanied by reduced accumulation of ICAM-1 at sites of neutrophil attachment, it did not affect adhesion of neutrophils to the endothelial cell surface (Yang et al., 2006a,b). In contrast to these results that suggest that endothelial cortactin may help

neutrophils to move through the endothelial barrier, other studies reported that cortactin seems to support the stabilization and closing of the endothelial barrier, as found for the barrier-enhancing effects of sphingosine-1-phosphate (S1P) and ATP on endothelial monolayers (Dudek et al., 2004; Jacobson et al., 2006). A role of cortactin for the maintenance of endothelial barrier integrity was not detected in these studies.

In this study, we have analyzed in vivo whether cortactin is relevant for the barrier function of endothelial cells. For this purpose, we generated and analyzed cortactin-deficient mice.
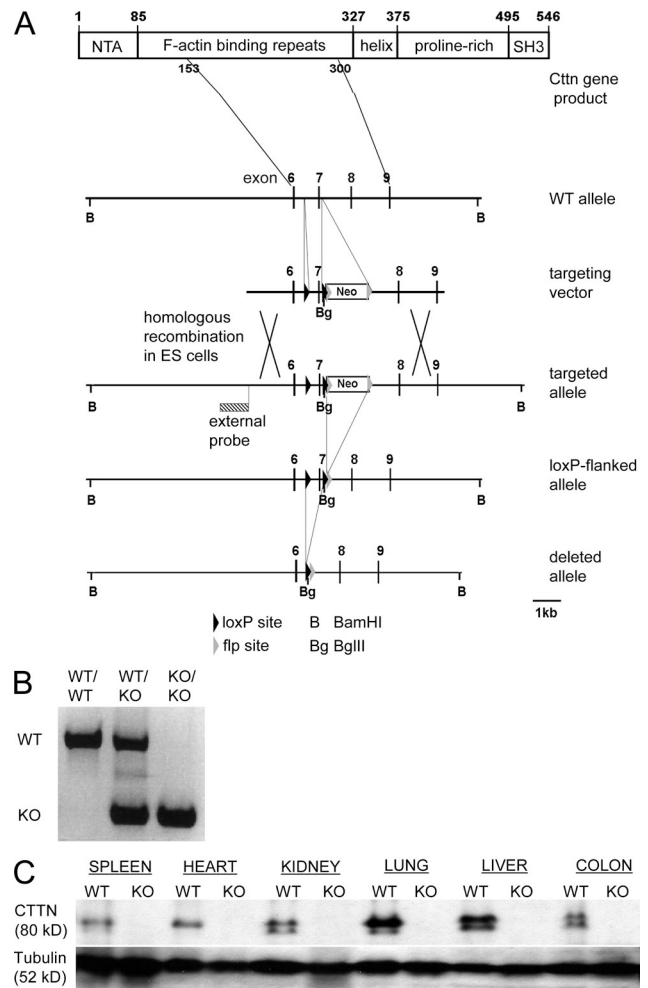

Figure 1. **Generation of cortactin–deficient mice.** (A) Domain organization of the cortactin protein and gene targeting strategy showing the partial genomic organization of the *Cttn* locus in WT, targeted, *loxP*-flanked (floxed), and deleted alleles. The vector carrying a neomycin resistance cassette (described previously in Lai et al. [2009]) to target the WT cortactin allele by homologous recombination in murine ES cells is depicted. Targeted ES cells were injected into blastocysts as described in Materials and methods. (B) PCR genotyping of mice carrying the WT and deleted (KO) alleles after consecutive crosses with mice expressing Flp and Cre recombinase. The top and bottom bands indicate the presence of WT *Cttn* allele (WT) and the deleted allele (KO), respectively. (C) Western blot analysis of different organ lysates derived from WT or cortactin-deficient mice (KO).

We analyzed the blood vessel barrier function with respect to neutrophil extravasation and vascular permeability for large molecular weight substances. We found that neutrophil extravasation into the TNF-stimulated cremaster was strongly reduced. Unexpectedly, this was caused by impaired neutrophil endothelial interactions as documented by increased rolling velocity and reduced leukocyte adhesion. Neutrophil rolling and firm adhesion were both supported by cortactin via β_2-integrin ligands. In contrast to the reduction of leukocyte extravasation, cortactin deficiency enhanced basal vascular permeability.

RESULTS

Generation and characterization of cortactin–deficient mice

To investigate the physiological role of cortactin, we used a conditional gene ablation approach by flanking exon 7 with loxP sites. The targeting vector was described previously (Lai et al., 2009), and the gene targeting strategy is outlined in Fig. 1 A. Consecutive crosses with mice systemically expressing Flp (to remove the neo-cassette) and Cre recombinase were performed to produce the null mutation on a mixed genetic background. Mice homozygous for the null mutation were successfully obtained by crossing mice with genotype del/WT. Deletion of exon 7 in the cortactin gene by Cre recombinase expressed in oocytes was expected to stop the reading frame generating a null allele in all cells of the organism. PCR genotyping of tail DNA samples revealed successful deletion of exon 7 (Fig. 1 B), and immunoblotting confirmed the absence of cortactin protein in homozygous del/del animals (KO) in any organ analyzed, as expected (Fig. 1 C). Using fibroblasts derived from double-targeted embryonic stem (ES) cells, in which deletion of exon 7 was induced in a comparable fashion in vitro, RT-PCR with primer pairs corresponding to regions of the 5′ end and the 3′ end of the cortactin message did not reveal any detectable cortactin transcript, as shown by Lai et al. (2009).
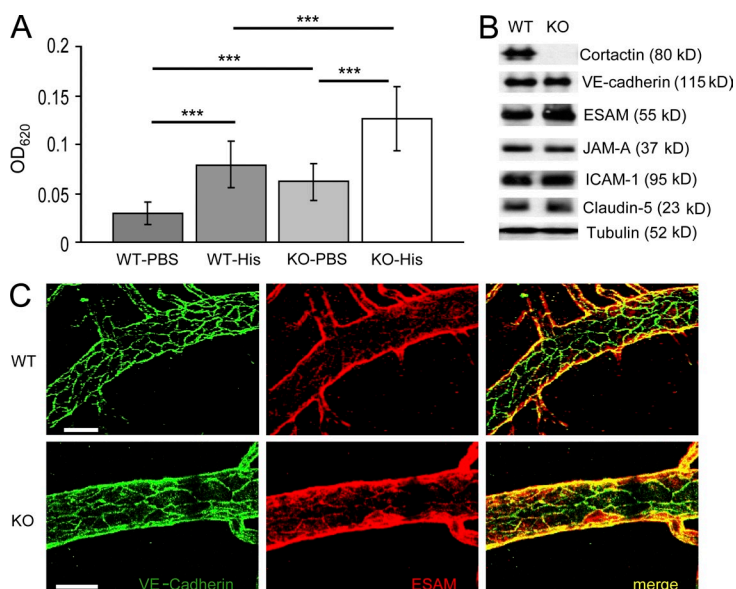
In a specific pathogen-free environment, adult *Cttn$^{WT/del}$* mice in a mixed genetic background were backcrossed with C57BL/6 mice. *Cttn$^{del/del}$* mice of the sixth backcross were used in our experiments. *Cttn$^{del/del}$* mice of mixed genetic background and of the sixth backcross showed no obvious phenotype, were healthy by visual inspection, and had a normal life span. Thus, cortactin is not essential for normal development, and its absence does not cause any obvious defects under specific, pathogen-free conditions.

Breeding *Cttn$^{WT/del}$* mice on a mixed 129Sv/C57BL/6 background generated homozygous *Cttn$^{del/del}$* mice with normal Mendelian frequency (Table S1), although we found a significant preference toward female offspring. When heterozygous mice of the sixth backcross (C57BL/6) were mated, *Cttn$^{del/del}$* mice were clearly underrepresented among the offspring (Table S2). The reason for this is currently unknown.

Loss of cortactin leads to increased vascular permeability in vivo

Based on RNA silencing in cultured endothelial cells, it has been suggested that cortactin is required for the enhancement of endothelial cell contact integrity by S1P or ATP; however, basal barrier integrity was unaffected (Dudek et al., 2004; Jacobson et al., 2006). This prompted us to use the Miles assay to test whether cortactin gene deficiency would affect vascular permeability in the skin. To this end, we injected WT and *Cttn$^{del/del}$* mice i.v. with Evans blue followed by intradermal injection of either histamine or PBS 15 min later. Remarkably, in the absence of any permeability-stimulating factor, the permeability in *Cttn$^{del/del}$* mice was more than twofold higher than in WT mice (Fig. 2 A), clearly demonstrating that cortactin controls basal permeability. Stimulation with histamine resulted in an additional increase of permeability in *Cttn$^{del/del}$* mice as compared with WT mice (Fig. 2 A). We conclude that cortactin is required in vivo to maintain basal barrier integrity within blood vessels.

To test whether the composition of membrane proteins at endothelial cell contacts would be disturbed in cortactin–deficient mice, we first analyzed the overall expression levels of vascular endothelial cadherin (VE-cadherin), endothelial cell–selective adhesion molecule (ESAM), JAM-A (junctional adhesion molecule A),

Figure 2. Cortactin deficiency leads to increased vascular permeability in vivo. (A) *Cttn$^{del/del}$* and *Cttn$^{WT/WT}$* mice were injected i.v. with Evans blue and 10 min later intradermally with histamine or PBS alone. Animals were sacrificed after an additional 30 min, and the dye was extracted from skin samples and quantified. Data are presented as means $\pm$ SD. $n = 12$ (WT); $n = 11$ (KO). ***, $P < 0.001$. Four independent assays with three to four mice per group were performed. (B) Lung lysates from *Cttn$^{del/del}$* (KO) and *Cttn$^{WT/WT}$* (WT) mice were analyzed by Western blot and probed for the indicated proteins. A representative blot from three independent experiments is shown. (C) Whole mount stainings of cremaster muscles from *Cttn$^{del/del}$* (KO) and *Cttn$^{WT/WT}$* (WT) mice for VE-cadherin and ESAM. Images are representative for three independent preparations each. Bars, 50 μm.

claudin-5, and also ICAM-1 in Western blots of the lung. As shown in Fig. 2 B, no difference was found in comparison with WT mice. Likewise, junctional localization of VE-cadherin and ESAM was unaffected by cortactin gene disruption, as shown by whole mount stainings of venules in the cremaster (Fig. 2 C). Relative pixel intensity in venules of the KO tissue was $107.9 \pm 12.7\%$ for ESAM and $102.9 \pm 8.7\%$ for VE-cadherin with pixel intensity for the WT values set to 100%. Isolation of primary endothelial cells from lungs of $Cttn^{del/del}$ mice and $Cttn^{WT/WT}$ mice (murine lung endothelial cells [MLECs]) allowed us to compare constitutive cell surface expression levels of VE-cadherin, ESAM, JAM-A, and PECAM-1 and expression of TNF-induced ICAM-1, VCAM-1 (vascular cell adhesion molecule 1), E-selectin, and P-selectin by flow cytometry. Each of these adhesion molecules was expressed at similar levels on both cell types (Fig. S1).

Inhibiting the expression of cortactin affects Rap-1 (Ras-related protein 1) activation and endothelial cell contact integrity

To elucidate the mechanism whereby cortactin supports cell contact integrity, we established siRNA-mediated down-regulation of the expression of cortactin in cultured human and mouse endothelial cells. Cortactin expression could be inhibited by 89% in human umbilical vein endothelial cells (HUVECs; Fig. 3 A) and by 81% in bend.3 mouse endothelioma cells (Fig. S4). Suppression of cortactin expression was accompanied by a 29.8% ($\pm 8.6\%$) increase of paracellular flux of 250-kD FITC-dextran across the monolayer of HUVECs grown on transwell filters (Fig. 3 C). Similar results were obtained for bend.3 mouse endothelioma cells (Fig. S4). Confluent monolayers of $Cttn^{del/del}$ MLECs had 68% ($\pm 23\%$) higher permeability than $Cttn^{WT/WT}$ MLECs for 250 kD FITC-dextran and 19% ($\pm 4\%$) enhanced permeability for 150-kD FITC-dextran (Fig. 3 E). In line with this, we found a 53% ($\pm 6.3\%$) reduction of transendothelial resistance of HUVEC monolayers (Fig. 3 D), confirming our in vivo finding that cortactin is indeed required for maintaining endothelial cell contact integrity.

Because it was shown before that activation of the Epac (exchange protein directly activated by cAMP)/Rap-1 pathway leads to stabilization of endothelial cell contacts (Cullere et al., 2005; Kooistra et al., 2005), we tested whether down-regulation of the expression of cortactin affects the levels of GTP-loaded Rap-1. Indeed, siRNA-mediated silencing of cortactin reduced the levels of activated Rap-1 by 41.7% ($\pm 9.4\%$) in HUVECs (Fig. 4 A) and by 74% ($\pm 17\%$) in bend.3 cells (Fig. S4). Likewise, levels of activated Rap1 were reduced by 51% ($\pm 6.7\%$)% in $Cttn^{del/del}$ MLECs compared with $Cttn^{WT/WT}$ MLECs (Fig. 4 A). Thus, cortactin is required to maintain the steady-state levels of GTP loading of Rap1.

Stimulating Epac/Rap-1 compensates the loss of cell contact integrity caused by down-regulation of cortactin

To test whether the reduction of Rap1 activation levels could explain why the loss of cortactin destabilizes endothelial cell

contacts, we investigated whether activation of Rap1 reverses the cortactin knockdown effect on endothelial permeability. To this end, we stimulated HUVECs with the cAMP analogue
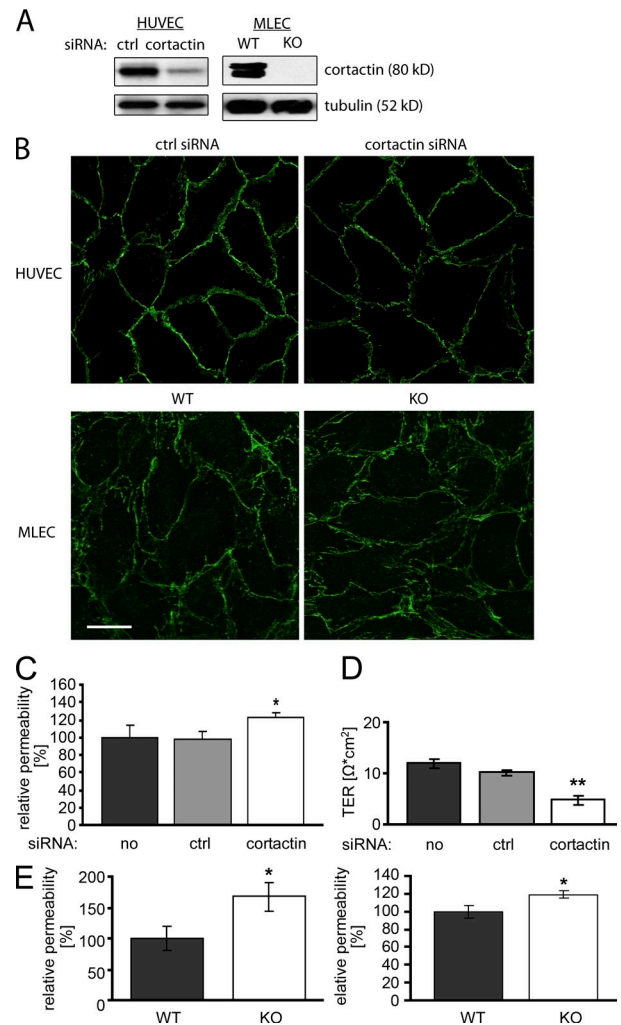
Figure 3. **Silencing or deficiency of cortactin enhances permeability of cultured endothelial cell layers.** (A) HUVECs were transfected with either control (ctrl) or cortactin-specific siRNAs. 48 h later, cell lysates were immunoblotted for cortactin expression (top). Cortactin immunoblots of primary MLECs isolated from $Cttn^{WT/WT}$ (WT) and $Cttn^{del/del}$ (KO) mice are shown. Equal loading was controlled by blotting for tubulin (bottom). Blots are representative of four independent experiments. (B) Micrographs of HUVEC monolayers transfected with control and cortactin siRNA and MLEC monolayers of $Cttn^{WT/WT}$ (WT) and $Cttn^{del/del}$ (KO) mice grown on transwell filters parallel to the experiment shown in C–E stained for VE-cadherin. Images are representative of four independent experiments. Bar, 20 µm. (C) Paracellular permeability for 250-kD FITC-dextran was determined for HUVECs transfected without oligonucleotides (set to 100%) or with either control or cortactin-specific siRNAs cultured on transwell filters (0.4-µm pore size). (D) Measurement of transendothelial electrical resistance (TER) of HUVECs treated as described in C. (E) Paracellular permeability of MLECs from $Cttn^{WT/WT}$ (WT) and $Cttn^{del/del}$ (KO) mice for 250 kD (left) and 150 kD FITC-dextran (right). (C–E) All data are means ± SD. $n = 6$ for each group in three independent experiments. *, $P < 0.05$; **, $P < 0.005$.

8-pCPT-2Me-cAMP (8-(4-Chlorophenylthio)-2'-O-methyl-cAMP; or 007) known to specifically activate the GTPase exchange factor Epac and thereby Rap1. As shown in Fig. 4 C, 8-pCPT-2Me-cAMP treatment of HUVECs transfected with cortactin–specific siRNA completely compensated the increase of FITC-dextran permeability caused by cortactin siRNA. In fact, the cAMP analogue reduced permeability to the same level in cortactin knockdown and control HUVECs. Similar results were obtained for bend.3 mouse endothelioma cells (Fig. S4) and for primary *Cttn^{del/del}* MLECs (Fig. 4 D and Fig. S5). This reveals that direct stimulation of Epac/Rap1 can stabilize cell contacts, and this is independent of cortactin function. In agreement with this, direct stimulation of Epac/Rap1 with 007 was not affected by the loss of cortactin in HUVECs or MLECs (Fig. 4 B). Because the loss of cortactin in turn leads to reduced activation levels of Rap1, our results position Epac/Rap1 downstream of cortactin.

Loss of cortactin inhibits neutrophil recruitment in vivo

The impairment of the vascular barrier function in cortactin-deficient mice prompted us to test whether this would also affect the extravasation of leukocytes. Analyzing TNF–inflamed cremaster tissue by intravital microscopy, we found that despite the loss of barrier integrity, neutrophil extravasation was not enhanced. Instead, it was strongly reduced by 50.8% (±22.8%; Fig. 5 D). Analyzing neutrophil rolling and firm adhesion, we found that the defect in extravasation was caused by impaired interactions of neutrophils with the vessel wall. Neutrophil rolling velocity was increased by 69.5% (±26.7%) in *Cttn^{del/del}* mice when compared with WT mice (Fig. 5 A), and the rolling flux fraction was increased by 105% (±27.6%; Fig. 5 B). In line with these results, the number of neutrophils that firmly adhered to the endothelium was reduced by 40.6% (±23.4%) in *Cttn^{del/del}* mice compared with littermate controls (Fig. 5 C). Hemodynamic parameters of the analyzed vessels are given in Table I, and representative videos are shown in the supplemental material

(Videos 1 and 2). We conclude that the slowing down of rolling neutrophils was less efficient in *Cttn^{del/del}* mice leading to faster rolling cells and a defect in neutrophil arrest. Because of this defect, cells continued to roll instead of stopping as firmly adhering cells, leading to increased numbers of rolling cells at the expense of firmly adhering cells. Thus, cortactin is required for optimal neutrophil extravasation efficiency at a step upstream of the actual transmigration process.

To determine whether cortactin acts in endothelial cells or in neutrophils during the extravasation process, we first analyzed whether it is expressed in neutrophils. In agreement with a previous study that reported the absence of cortactin in all bone marrow–derived cells except megakaryocytes (Zhan et al., 1997), we could not detect cortactin in immunoblots of mouse leukocyte lysates (Fig. S2). However, this did not rule out the possibility that low expression levels of cortactin below detection levels might be sufficient to support functions relevant for leukocyte extravasation. To test this, we generated chimeric mice by irradiating WT mice and transplanting them with bone marrow cells from either *Cttn^{del/del}* mice or (as controls) from *Cttn^{WT/WT}* littermates. Intravital microscopy of the TNF–inflamed cremaster of these mice revealed no differences in rolling velocity, rolling flux fraction, or in the number of adherent or extravasated neutrophils when compared with WT mice transplanted with WT bone marrow (Fig. 5, E–H). These results formally rule out the possibility that cortactin potentially expressed below detection limit in neutrophils participates in their extravasation. In addition, these experiments exclude the possibility that platelets, which do express cortactin (Vidal et al., 2002) and are known to be important for neutrophil recruitment into inflamed tissue (Bixel et al., 2010), would require cortactin for their participation in neutrophil extravasation.

Importantly, cortactin gene disruption did neither reduce peripheral leukocyte counts nor cause any changes in the repertoire of leukocyte surface molecules relevant for leukocyte
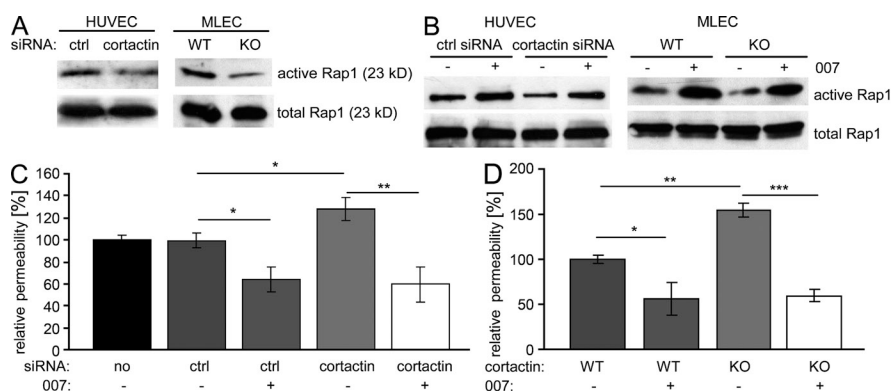
Figure 4. Loss of cortactin leads to decreased levels of active Rap1, and Epac activation fully compensates the effect on permeability caused by down–regulation of cortactin. (A) Western blot analysis of pull-down assays for active Rap1 in HUVECs transfected with either control (ctrl) or cortactin-specific siRNA and for primary MLECs from *Cttn^{WT/WT}* (WT) and *Cttn^{del/del}* (KO) mice. Total Rap1 levels were controlled by blotting aliquots of the whole cell lysates from which the pull-downs were performed. (B) Rap1 activation assays as in (A) performed with HUVECs transfected with either control or cortactin-specific siRNA or of MLECs from *Cttn^{WT/WT}* (WT) and *Cttn^{del/del}* (KO) mice and additionally treated with 100 µM 8-pCPT-2Me-cAMP (+007) or vehicle (−007). (A and B) The depicted immunoblots are representative of three similar experiments. (C) Permeability for 250-kD FITC-dextran was analyzed in HUVECs transfected with either control or cortactin-specific siRNA and treated with either 100 µM 8-pCPT-2Me-cAMP (007) or vehicle. (D) Permeability for 250-kD FITC-dextran was analyzed in MLECs from *Cttn^{WT/WT}* (WT) and *Cttn^{del/del}* (KO) mice as described for HUVECs in C. (C and D) Graphs are representative of three independent experiments. All data are presented as mean ± SD. *, P < 0.05; **, P < 0.01; ***, P < 0.001.

extravasation. Indeed, we did find a slight tendency toward higher numbers of neutrophils and lymphocytes in the blood of *Cttn*[del/del] animals compared with WT controls; however, the differences were not statistically significant (Fig. S2). Furthermore, neither platelet nor erythrocyte counts were significantly affected by cortactin gene disruption. In addition, surface expression of L-selectin, PSGL-1 (P-selectin glycoprotein ligand 1), Gr-1, CD11a, CD11b, CD44, and CXCR2 was not affected by the systemic loss of cortactin (Fig. S2). Collectively, our results suggest that it is the lack of endothelial

Figure 5.   Cortactin is required for leukocyte rolling, adhesion, and transmigration in vivo. (A–D) The velocity of rolling cells (A), the rolling flux fraction (B), the number of firmly adherent cells (C), and the number of transmigrated cells (D) were investigated by intravital video microscopy and reflected light oblique transillumination microscopy of cremaster muscle venules of *Cttn*[del/del] (KO) and *Cttn*[WT/WT] (WT) mice. Inflammation was induced by intrascrotal injection of 500 ng TNF 3 h before analysis. The results are displayed as mean ± SD of at least 20 vessels from four different animals in each group. ***, P < 0.0005. (E–H) Chimeric mice generated by transplanting bone marrow from WT animals or from cortactin-deficient mice (KO) into lethally irradiated WT mice were analyzed by intravital microscopy of cremaster as for A–D. The velocity of rolling cells (E), the rolling flux fraction (F), the number of firmly adherent cells (G), and the number of transmigrated cells (H) were determined and showed no significant differences between the two types of chimeras. Results were obtained from three mice per group. (I) Leukocyte rolling velocity in venules of TNF-stimulated cremaster was determined as in A and E from *Cttn*[del/del] (KO) and *Cttn*[WT/WT] (WT) mice that had been injected with a combination of anti–LFA-1 and anti–Mac-1 blocking antibodies (30 µg of each per mouse) just before cremaster muscle exteriorization. No-antibody controls are shown in A. Results were determined from four mice per group.

cortactin that impairs leukocyte extravasation in cortactin-deficient mice.
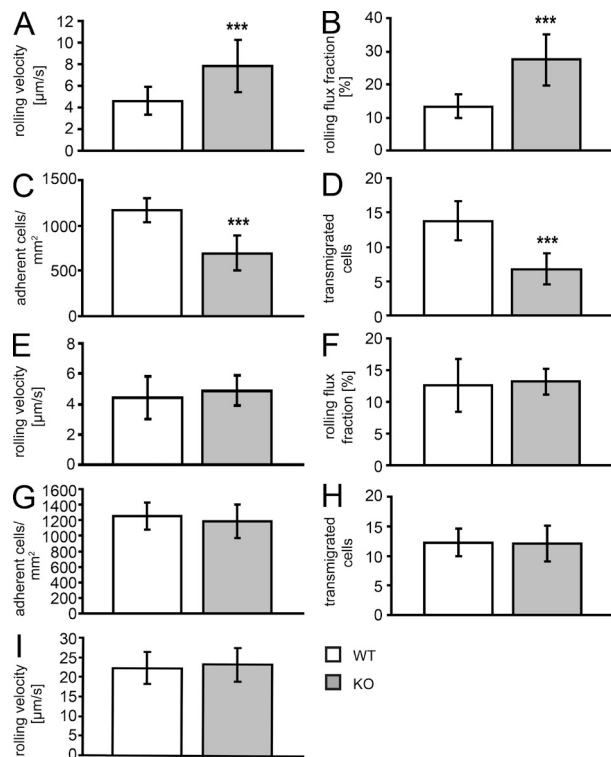
Cortactin deficiency impairs the ability of endothelial β₂-integrin ligands to slow down leukocyte rolling

Leukocyte rolling is initiated by the endothelial selectins and slowed down by the binding of the β_2-integrins LFA-1 (lymphocyte function–associated antigen 1) and Mac-1 (macrophage 1 antigen) to their endothelial ligands (Kunkel et al., 2000; Dunne et al., 2002). Thus, the enhanced leukocyte rolling velocity in cortactin-deficient mice could have either been caused by impaired selectin-mediated rolling or by the inability of endothelial β_2-integrin ligands to slow down leukocyte rolling. To test the second possibility, we determined whether cortactin deficiency would still affect the rolling velocity when LFA-1 and Mac-1 are simultaneously blocked with antibodies. As shown in Fig. 5 I, we found that blocking LFA-1 and Mac-1 resulted in the expected strong increase in rolling velocity in *Cttn*[WT/WT] mice. Importantly, these antibodies had no further effect on the rolling velocity in *Cttn*[del/del] mice compared with *Cttn*[WT/WT] mice (Fig. 5 I). This demonstrates that the lack of cortactin did no longer enhance the rolling velocity if only the endothelial selectins but not the β_2-integrins were available to support rolling. This suggests indirectly that cortactin supports neutrophil rolling via β_2-integrin ligands and not via endothelial selectins.

Cortactin is required for proper functioning of ICAM-1 in neutrophil extravasation

Our intravital microscopy results (Fig. 5) suggest that the defect in neutrophil extravasation in cortactin-deficient mice is caused by impaired neutrophil rolling and firm adhesion. To investigate how cortactin could affect transmigration, we decided to test whether we can recapitulate this effect in vitro. To exclude the rolling aspect, we performed static transmigration assays with endothelial cell monolayers grown on transwell filters. In agreement with the in vivo results, cortactin siRNA inhibited transmigration of human neutrophils through HUVEC monolayers by 36% (Fig. 6 A) and of mouse neutrophils through bend.5 cell layers by 40% (Fig. S4). Likewise, transmigration of mouse neutrophils through monolayers of primary MLECs isolated from *Cttn*[del/del] mice was reduced by 49% in comparison with MLECs from *Cttn*[WT/WT] mice (Fig. 6 B). Neutrophils adhered to *Cttn*[del/del] MLECs with similar efficiency (51.8 ± 4.1% of applied PMNs) as to *Cttn*[WT/WT] MLECs (52.9 ± 6.8% of applied PMNs), possibly reflecting the fact that assays were performed under static conditions.

Because ICAM-1 is the major endothelial adhesion receptor relevant for firm neutrophil binding, we tested whether cortactin would influence neutrophil transmigration via ICAM-1. If this was the case, knockdown of cortactin expression would have no inhibitory effect on neutrophil transmigration in endothelial cells lacking ICAM-1. To test this hypothesis, we used mouse endothelioma cells deficient for ICAM-1 and, as a control, the same cells retransfected for ICAM-1. Expression levels of cortactin in these endothelioma

Table I. Hemodynamic parameters of cortactin-deficient and WT littermate mice

Genotype	Venules	Diameter	Centerline velocity	Wall shear rate
		μm	*mm/s*	*1,000/s*
Cortactin[WT/WT]	26	36.8 ± 4.7	3.65 ± 0.1	1.02 ± 0.18
Cortactin[del/del]	22	30.3 ± 7.3[a]	3.67 ± 0.11	1.31 ± 0.31[a]

Data are presented as mean ± SD of all examined venules.
[a]$P < 0.01$.

cells were similar to bend.3 or bend.5 cells (not depicted), and siRNA transfection reduced cortactin expression by 87% in ICAM-1–deficient cells and by 83% in ICAM-1–retransfected cells (Fig. 6 D).

As shown in Fig. 6 E, ICAM-1 deficiency reduced neutrophil transmigration by 70% (±25.8%). Inhibition of cortactin expression in these ICAM-1–deficient endothelial cells did not inhibit neutrophil transmigration any further, whereas in ICAM-1 retransfectants, cortactin siRNA inhibited neutrophil transmigration by 31.2 ± 8.4%. Thus, in the absence of ICAM-1, cortactin does not contribute to neutrophil transendothelial migration, suggesting that cortactin acts by supporting ICAM-1 functions.

Neutrophil transmigration through endothelial cell layers is accompanied by the clustering of ICAM-1 around adhering leukocytes, which strengthens cell adhesion and thereby facilitates the transmigration process (Barreiro et al., 2002; Carman et al., 2003). Therefore, we tested whether ICAM-1 clustering would be dependent on the expression of cortactin.

We observed in control-transfected HUVECs ICAM-1–enriched ring-like structures surrounding adherent neutrophils. Cortactin was also enriched in these structures, partly colocalizing with ICAM-1 (Fig. 7 A). Importantly, after down-regulation of cortactin expression by siRNA, only very few of such structures were still observed, and the vast majority of neutrophils were devoid of these rings (Fig. 7 A). We quantified the effect on the formation of ICAM-1–containing rings at sites of neutrophil contact (Fig. 7 B). More than 79% of PMNs on cortactin-positive cells showed closed ICAM-1–positive ring structures, whereas 21% of adherent cells on cortactin-positive HUVECs were not surrounded by such structures. The situation was completely different for PMNs
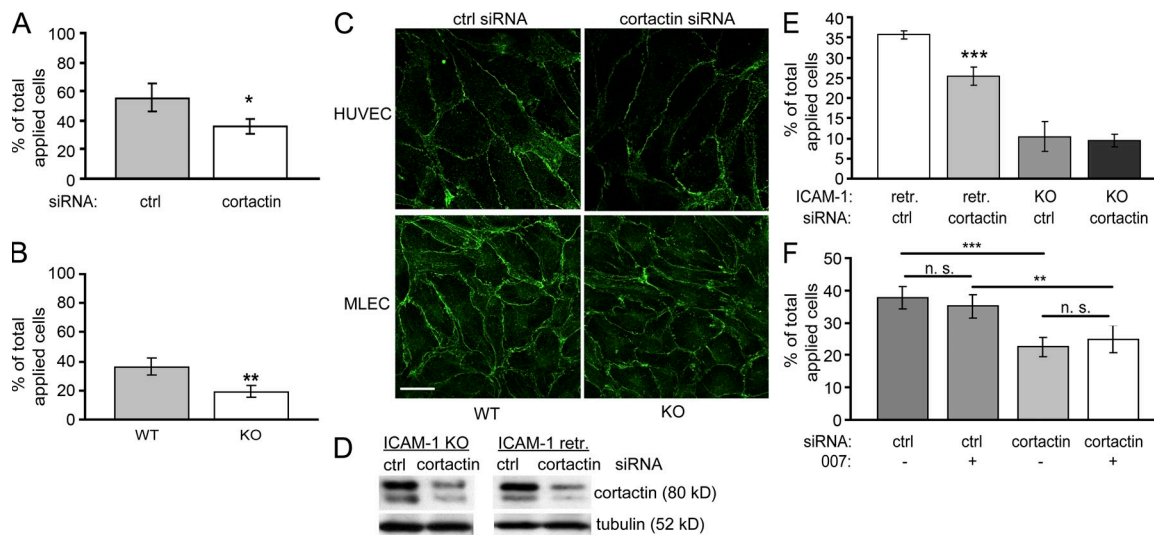
Figure 6. Loss of cortactin causes an ICAM–1–dependent reduction of leukocyte transmigration. (A) Human primary neutrophils were allowed to transmigrate through a TNF-activated monolayer of HUVECs on transwell filters (5-μm pore size) transfected with either control (ctrl) or cortactin-specific siRNAs. (B) Transmigration of mouse PMNs through a TNF-activated monolayer of MLECs from *Cttn*[WT/WT] (WT) and *Cttn*[del/del] (KO) mice on transwell filters (3-μm pore size). The amount of transmigrated neutrophils is displayed as the percentage of total applied cells. (C) Micrographs of HUVECs transfected with control and cortactin siRNA or of MLECs from *Cttn*[WT/WT] (WT) and *Cttn*[del/del] (KO) mice, grown on transwell filters parallel to the experiments shown in A and B and stained for VE-cadherin. Bar, 20 μm. (A–C) Experiments were independently performed three times. (D) ICAM-1–deficient (KO) and ICAM-1–retransfected (retr.) endothelioma cells were transfected with either control or cortactin-specific siRNAs. 48 h later, cell lysates were immunoblotted for cortactin expression (top). Equal loading was controlled by blotting for tubulin (bottom). (E) Bone marrow–derived murine PMNs were allowed to transmigrate across TNF-activated ICAM-1–deficient (KO) and ICAM-1–retransfected endothelioma cell lines transfected with either control or cortactin-specific siRNA. (D and E) Experiments were performed three times. (F) Transmigration of human PMNs through HUVEC monolayers transfected with either control or cortactin-specific siRNA and additionally treated with either 100 μM 8-pCPT-2Me-cAMP (+007) or vehicle (−007). (A, B, E, and F) All data are means ± SD. *, $P < 0.05$; **, $P < 0.01$; ***, $P < 0.005$ ($n = 6$ in three independent experiments; n.s., not significant).
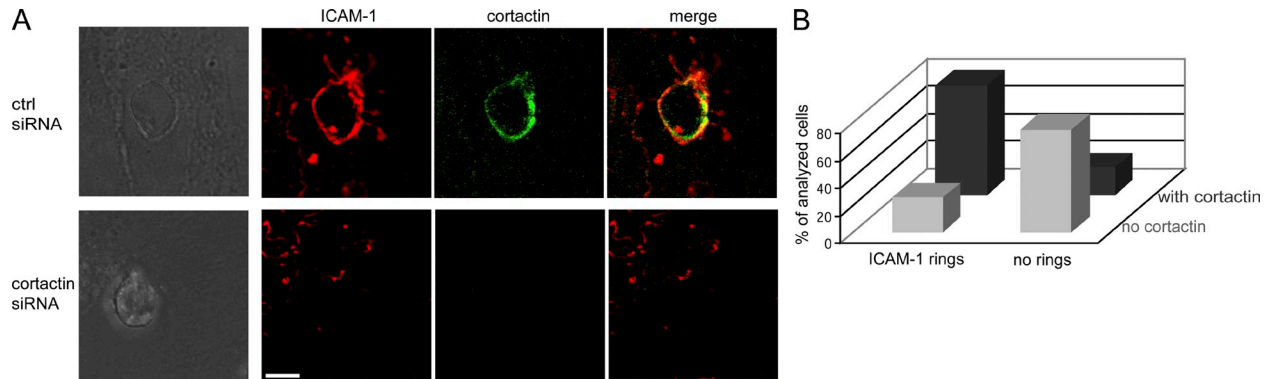
Figure 7.   Reduced leukocyte transmigration after down–regulation of cortactin is accompanied by impaired formation of ICAM–1 clusters. HUVECs were incubated for 20 min with human primary PMNs as described in Materials and methods followed by fixation and immunofluorescence microscopy. (A) HUVECs transfected with control (ctrl) siRNA show ICAM-1 (red) and cortactin (green) containing ring structures surrounding a PMN. HUVECs transfected with cortactin-specific siRNA show no ICAM-1 clustering around the PMN. Associated leukocytes were visualized by transmitted light (left). Bar, 5 µm. (B) Apically adherent PMNs from randomly selected fields of three independent experiments were scored for the presence of ICAM-1–containing ring structures. A representative experiment with the percentage of analyzed cells is displayed. A total of 112 PMNs (on cortactin-depleted HUVECs) and 119 PMNs (on cortactin-positive HUVECs) were analyzed.

in contact with cortactin-depleted HUVECs. Here, only 25% showed ICAM-1–positive ring structures, and 75% of these cells showed no ICAM-1 rings. These results demonstrate that the presence of cortactin is required for proper formation of ICAM-1–enriched clusters around adhering PMNs, thus allowing for correctly regulated neutrophil recruitment.

To test whether the lack of cortactin would impair neutrophil transmigration via the reduced level of activated Rap1, we tested whether the specific activator 8-pCPT-2Me-cAMP (007) of Epac/Rap1 would affect transmigration of human PMNs through HUVEC monolayers either treated with control siRNA or with cortactin siRNA. As shown in Fig. 6 F, 007 had no effect on neutrophil transmigration, suggesting that Rap1 is not involved in mechanisms whereby cortactin supports neutrophil extravasation.

Cortactin is required for ICAM-1–triggered activation of RhoG

RhoG has recently been reported to be required for the formation of leukocyte-surrounding ICAM-1 clusters and leukocyte transmigration (van Buul et al., 2007). The activation of RhoG was found to be triggered by leukocyte engagement of ICAM-1. This prompted us to test whether RhoG activation would be compromised in $Cttn^{del/del}$ MLECs. Therefore, we incubated primary isolated MLECs of $Cttn^{WT/WT}$ and $Cttn^{del/del}$ mice with beads either loaded with antibodies against mouse ICAM-1 or with control antibodies and performed RhoG activation assays using the effector protein ELMO (engulfment and cell motility gene) in pull-down experiments. As shown in Fig. 8, engagement of ICAM-1 triggered activation of RhoG in $Cttn^{WT/WT}$ but not in $Cttn^{del/del}$ MLECs. Thus, cortactin is required for ICAM-1–triggered activation of RhoG, a signaling process involved in the transmigration of neutrophils.

Constitutively active (CA) RhoG restores Cttn$^{del/del}$ defects in transmigration

To determine whether the defect in ICAM-1–triggered RhoG activation in $Cttn^{del/del}$ MLECs would be responsible for impaired neutrophil transmigration, we tested whether transfection of CA-RhoG would rescue the phenotype. We found that CA-RhoG but not WT RhoG indeed partially restored the formation of ICAM-1–containing rings around neutrophils adhering to $Cttn^{del/del}$ MLECs (Fig. 8 B). In addition, transmigration efficiency of neutrophils across a monolayer of these cells was largely restored with CA-RhoG (Fig. 8 C). We conclude that the defect in ICAM-1–triggered activation of RhoG is responsible for impaired ICAM-1 clustering and neutrophil transmigration in cortactin-deficient endothelial cells.

DISCUSSION

Analyzing cortactin-deficient mice, we show for the first time that this actin-remodeling protein is required in endothelial cells, not in neutrophils, for optimal efficiency of neutrophil recruitment to inflamed tissue. Loss of cortactin caused an increase in rolling velocity and a decrease of neutrophil adhesion to the vessel wall. Thus, endothelial cortactin is required for slowing down rolling neutrophils and for firm adhesion to the vessel wall. Interestingly, cortactin was not required for the support of selectin-mediated rolling but for the slowing down of rolling mediated by β_2-integrins and their ligands. In addition, formation of ICAM-1–containing clusters was disturbed, providing a possible explanation for the decreased numbers of neutrophils adhering to the vessel wall. Searching for a mechanism for this defect, we found that cortactin deficiency blocked the activation of RhoG triggered by ICAM-1 engagement, and CA-RhoG partially restored ICAM-1 clustering and neutrophil transmigration across cortactin-deficient endothelial cells. Independent of the role
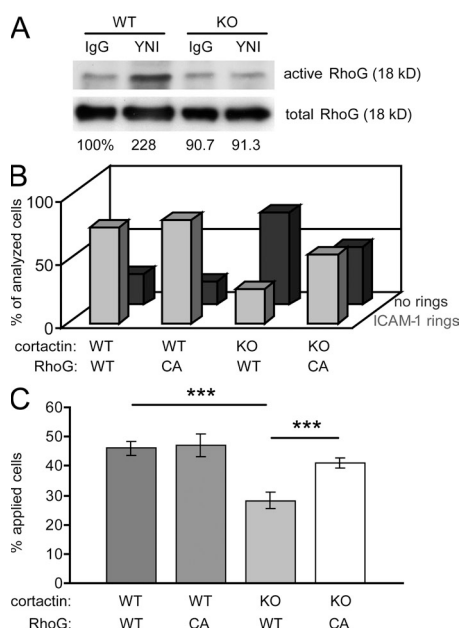
of cortactin in neutrophil extravasation, we found that cortactin is essential to maintain endothelial cell contact integrity. Gene deficiency led to enhanced basal permeability for high molecular weight substances. This effect could be rescued by directly activating Epac/Rap1 with a stable cAMP derivative, suggesting that cortactin acts upstream of Rap1. Thus, cortactin affects leukocyte extravasation and endothelial cell contact integrity by controlling the activity of two different GTPases in two independent mechanisms.

Neutrophil capturing, rolling, and adhesion represent consecutive steps of a complex process that requires the interplay of selectins and neutrophil integrins. It is well documented that P- and E-selectin mediate capturing and rolling of neutrophils (Vestweber and Blanks, 1999). Besides directly mediating rolling via binding to various neutrophil selectin ligands (McEver, 2002; Hidalgo et al., 2007), the endothelial selectins intensify the rolling interactions and thereby slow down

Figure 8. Cortactin is required for ICAM–1–triggered activation of RhoG. (A) Primary MLECs isolated from $Cttn^{WT/WT}$ (WT) and $Cttn^{del/del}$ (KO) mice were incubated for 30 min with beads loaded with either control antibody (IgG) or the mAb YNI against ICAM-1. Active RhoG was pulled down from cell lysates with ELMO-GST and detected in immunoblots (top). Total RhoG levels subjected to pull-downs were controlled by blotting aliquots of the cell lysates (bottom). Quantification of signal intensity of the pulled down material is depicted below. (B) MLECs from $Cttn^{WT/WT}$ (WT) and $Cttn^{del/del}$ (KO) mice transfected with WT RhoG or CA-RhoG were incubated for 20 min with mouse PMNs followed by fixation and immunofluorescence microscopy for ICAM-1. 109 PMNs (on WT cells with WT RhoG), 102 PMNs (on WT cells with CA-RhoG), 81 PMNs (on KO cells with WT RhoG), and 92 PMNs (on KO cells with CA-RhoG) were analyzed for the presence of surrounding ICAM-1 rings. (C) Transmigration of mouse PMNs through a TNF-activated monolayer of MLECs from $Cttn^{WT/WT}$ (WT) and $Cttn^{del/del}$ (KO) mice transfected with WT RhoG or CA-RhoG. The amount of transmigrated neutrophils is displayed as the percentage of total applied cells. Data are presented as mean ± SD. ***, $P < 0.005$. (A–C) Experiments were independently performed three times.

rolling velocity by activating the neutrophil integrins LFA–1 and Mac–1, which participate in this process via binding to ICAM–1 and additional endothelial ligands (Kunkel et al., 2000; Dunne et al., 2002; Wang et al., 2007; Zarbock et al., 2007, 2008; Miner et al., 2008). Slowing down neutrophil rolling has so far only been studied as a neutrophil process requiring signaling that triggers integrin activation (Zarbock and Ley, 2009). We show here that also endothelial adhesion molecules require cytosolic components that are necessary to enable them to support neutrophil rolling. With cortactin, we have identified the first intracellular component in endothelial cells that is required in vivo for the slowing down of rolling neutrophils.

In vitro studies have suggested that E-selectin requires cytoskeletal components for its function. Various actin-associated proteins were copurified with E-selectin upon interaction with neutrophils (Yoshida et al., 1996), one of them being cortactin (Tilghman and Hoover, 2002). Although one study suggested that the cytoplasmic tail of E-selectin would be dispensable for the adhesive function of E-selectin (Kansas and Pavalko, 1996), another showed that clustering of E-selectin in either clathrin-coated pits or lipid rafts enhanced neutrophil adhesion under flow (Setiadi and McEver, 2008). Collectively, these results suggest that the cytoskeleton can influence E-selectin function. In this context, it is remarkable that cortactin deficiency, although clearly affecting rolling velocity in vivo, did not affect rolling when the function of β_2–integrins was blocked. Thus, cortactin only contributes to the rolling velocity if the integrins on PMNs are functional. This is indirect evidence suggesting that cortactin is required for the transition of fast to slow neutrophil rolling and this process depends on the adhesive function of β_2-integrin ligands. Of the three β_2-integrin ligands ICAM-1, ICAM-2, and JAM-A, only ICAM-1 has a clearly detectable although only small role in slow rolling (Ley et al., 1998; Steeber et al., 1998), whereas ICAM-2 seems not to serve as a rolling ligand of LFA-1 (Dunne et al., 2003) and JAM-A does not appear to play a role in adhesion under flow (Ostermann et al., 2002). It will be interesting to study in the future how cortactin participates in the incorporation of ICAM-1 and possibly other β_2-integrin ligands into the rolling process. Possibilities range from the support of ligand miniclusters or even selectin/integrin ligand heteroclusters to the organization of a cortical actin network that may provide a platform to stabilize forces that pull on ICAM-1 and/or other β_2-integrin ligands.

In addition to the contribution to neutrophil rolling, our results reveal that cortactin is also needed in vivo for firm adhesion of neutrophils in inflamed venules and for clustering of ICAM-1, which supports firm adhesion of leukocytes to endothelial cells and subsequent transmigration (Barreiro et al., 2002; Carman et al., 2003; Carman and Springer, 2004). Other cytoskeletal adaptors that are important for the formation of such structures are the ERM (ezrin, radixin, and moesin) proteins (Barreiro et al., 2002) and filamin B, which was found to be involved in ICAM-1 recruitment to adhering

leukocytes (Kanters et al., 2008). As a mechanism whereby cortactin deficiency impairs the formation of ICAM clusters and neutrophil transmigration, we found that cortactin is essential for the activation of RhoG, triggered by the engagement of ICAM-1 on the surface of endothelial cells. ICAM-1–triggered RhoG activation was recently demonstrated to be critical for the formation of ICAM-1 clusters and also for neutrophil transmigration (van Buul et al., 2007). Interestingly, neither the depletion of RhoG via siRNA (van Buul et al., 2007) nor cortactin deficiency (this study) impaired neutrophil adhesion to endothelial cells in static adhesion assays. In the light of our in vivo results, this suggests that ICAM-1–containing clusters affect neutrophil arrest only under in vivo flow conditions.

Our results are in agreement with studies by Yang et al. (2006a,b) who showed that cortactin supports the clustering of ICAM-1 into ring-like structures around neutrophils attached to HUVECs. However, although they found that silencing of cortactin inhibited neutrophil transmigration through endothelial cell layers under flow conditions, they found no effect on neutrophil adhesion to the apical surface of endothelial cells. Rolling velocity was not reported in these studies, and the fact that no inhibitory effects on neutrophil attachment were detectable might be caused by differences between in vitro and in vivo conditions, or not least to the fact that siRNA cannot block expression as completely as gene deficiency. Interestingly, however, the study by Yang et al. (2006b) and also our in vitro results may hint toward an additional function of cortactin downstream of neutrophil rolling and adhesion, which could be a role in the diapedesis process itself or in the initiation of this process. In the light of these results, it is important to note that ICAM-1 cross-linking triggers tyrosine phosphorylation of cortactin. This suggests that cortactin is involved in ICAM-1 signaling (Durieu-Trautmann et al., 1994), which is in good agreement with our finding that cortactin is required for ICAM-1–triggered activation of RhoG. ICAM-1 clustering triggers various signals that may be involved in the destabilization of endothelial junctions (Adamson et al., 1999; Etienne-Manneville et al., 2000; Allingham et al., 2007; Turowski et al., 2008). Whether cortactin participates in neutrophil diapedesis in vivo can currently not be decided because of its prominent role in neutrophil rolling and firm adhesion.

Our in vivo analysis of vascular permeability and also our in vitro results showed that cortactin is required to maintain the barrier function of the vasculature. Whereas our in vitro results clearly show that it is endothelial cortactin that is required for endothelial cell contact integrity, it is also possible that in vivo cortactin in perivascular cells may additionally contribute to the integrity of the vessel wall. Previous in vitro studies suggested that cortactin is required for signaling mechanisms that enhance the stability of endothelial cell contacts. Treatment of pulmonary endothelial cells with either S1P or ATP led to barrier enhancement via junctional translocation of cortactin accompanied by translocation and activation of Rac1 and MLCK (myosin light chain kinase; Dudek et al., 2004;

Jacobson et al., 2006). However, silencing of cortactin expression in these studies blocked S1P or ATP-stimulated enhancement of the barrier function but had no effect on the baseline permeability of cultured pulmonary endothelial cells. Thus, a requirement of cortactin for the maintenance of baseline barrier integrity as shown in our cortactin-deficient mouse model has not yet been described. Our findings that cortactin expression supports Rap1 activation and that stimulation of Epac/Rap1 with 8-pCPT-2Me-cAMP can rescue endothelial cell contact integrity in cells lacking cortactin suggests that Rap1 acts downstream of cortactin in the control of endothelial cell contact integrity. In contrast, it has been reported that activation of Epac/Rap1 by 8-pCPT-2Me-cAMP results in enhanced barrier integrity through improved VE-cadherin–dependent cell adhesion and increased cortical actin formation, which was accompanied by translocation of cortactin to cell junctions (Fukuhara et al., 2005; Kooistra et al., 2005). In addition, Epac/Rap1 activation was suggested to lead to Rac1 activation and translocation to cell junctions, which was accompanied by cortactin recruitment to endothelial junctions (Baumer et al., 2008). Thus, a positive feedback loop may exist where cortactin supports Rap1 activation and at the same time activated Rap1 stimulates the recruitment of more cortactin to cell contacts.

In numerous in vitro studies, cortactin has been implicated to be involved in many important cellular processes that require actin remodeling (e.g., Selbach and Backert, 2005; Ammer and Weed, 2008; Ren et al., 2009). Through physical interactions with actin filaments and the Arp2/3 complex, cortactin is thought to promote Arp2/3-dependent actin filament nucleation. However, whether the vascular phenotype of cortactin-deficient mice we describe here is indeed caused by a lack of a direct impact of cortactin on the actin cytoskeleton remains to be determined.

Recent studies investigating ES cell–derived fibroblasts harboring a null mutation analogous to the one used here or primary cells derived from independently generated cortactin-deficient mice consistently demonstrated a nonessential role for cortactin in actin remodeling (Lai et al., 2009; Tanaka et al., 2009). Although we found a slight induction of actin fibers that cross through the body of cortactin-deficient cells (Fig. S3), the nature of these fibers and potential functions are unclear. Instead of major effects on actin remodeling, cortactin was found to be involved in platelet-derived growth factor–induced signaling to Rho-GTPases (namely Rac-1 and Cdc42) and in cell migration (Lai et al., 2009). The data suggest that cortactin may operate in signaling to actin polymerization more indirectly than previously anticipated, possibly through contributing to the temporal and spatial regulation of activation of selected Rho GTPases. This is in good agreement with our results on the role of cortactin for the regulation of Rap1 and RhoG activity in endothelial cells.

Other cortactin-deficient mouse models have recently been presented with various phenotypes. Tanaka et al. (2009) generated mice homozygous for a cortactin allele devoid of

exon 5 and succeeded in isolating embryonic fibroblasts on embryonic day (E) 15 of development. Although it was not mentioned whether these mice are viable beyond E15, considering the results described here, such a scenario seems likely. In contrast, Yu et al. (2010) generated a cortactin-deficient mouse model using a gene-trap vector. Although they reported heterozygous animals being viable and fertile, they failed to obtain homozygous offspring. As an explanation for this defect, the authors concluded that cortactin plays a role in asymmetric division of oocytes. Although a lack of embryonic lethality in the mouse model described by Tanaka et al. (2009) remains to be experimentally demonstrated, it is tempting to speculate that the strong phenotype observed by Yu et al. (2010) may be explained, at least in part, by dominant-negative effects caused by expression of N-terminal cortactin residues fused to β-galactosidase in this gene-trap mutant. A potential role of cortactin in spermiogenesis was previously proposed by Kai et al. (2004) based on the analysis of mice (C57BL/6 × C3H mixed genotype) carrying a large genomic deletion including the cortactin locus. At least for mice of the genotype analyzed here (129SV × C57BL/6 mixed background and C57BL/6 sixth backcross), we can exclude this function for cortactin because our cortactin-deficient male mice are fertile.

In conclusion, our results establish cortactin as an essential physiological component of the molecular machinery that controls basal vascular permeability by supporting barrier integrity of the endothelium in vivo. In addition, cortactin is required for proper functioning of two types of ICAM-1–mediated endothelial–neutrophil interactions in vivo: the slow rolling of neutrophils, which depends on the contribution of ICAM-1, and the firm adhesion that is mediated by clustered ICAM-1. Thus, cortactin is crucial for stabilizing the endothelial barrier at endothelial cell contacts and supporting neutrophil accumulation at the luminal surface of the endothelium leading to neutrophil extravasation.

MATERIALS AND METHODS

Antibodies and reagents. The following commercial primary antibodies were used: monoclonal anticortactin (clone 4F-11; Millipore), polyclonal anticortactin (clone GK18; Sigma-Aldrich), anti–VE-cadherin (clone C19; Santa Cruz Biotechnology, Inc.), anti–ICAM-1 (clone R6-5-D6 [BioX-Cell]; clone YN1/1.7 [Takei, 1985]), anti–α-tubulin (clone B-5-1-2; Sigma-Aldrich), monoclonal anti-CD11a and anti-CD11b (clones M17/4 and M1/70; BD), and anti–PECAM-1 (clone MEC13.3; BioLegend). Antibodies against mouse P-selectin (clone RB40/34; Bosse and Vestweber, 1994), mouse E-selectin (clone UZ4; Hammel et al., 2001), mouse VE-cadherin (polyclonal serum C5 and clone 11D4), and ESAM (VE19) have been described previously (Gotsch et al., 1997; Nasdala et al., 2002). pAbs against JAM-A (Khandoga et al., 2009) and mAb against mouse VCAM-1 (Hahne et al., 1993) are as previously described. Fluorescently labeled secondary antibodies were purchased from Invitrogen. Peroxidase-labeled secondary antibodies were purchased from Dianova. F-actin was stained using Alexa Fluor 568–conjugated phalloidin (Invitrogen). Epac was activated using 8-pCPT-2Me-cAMP (Biolog). The mAb against RhoG and the expression construct for ELMO-GST were gifts of M.A. Schwartz (University of Virginia, Charlottesville, VA). ELMO-GST was purified from BL-21 bacteria using glutathione–Sepharose 4B (GE Healthcare) as described previously (Meller et al., 2008).

Generation of cortactin-deficient mice. Two independent targeting vectors harboring neomycin and puromycin cassettes, respectively, were previously used to allow consecutive targeting of both cortactin alleles in ES cells that were then injected into blastocysts giving rise to chimeric embryos that were used to isolate puromycin- and neomycin-resistant fibroblast cultures (Lai et al., 2009). To generate cortactin-deficient mice, ES cells (line IGD3.2) were modified by homologous recombination of only one allele with the neomycin-containing construct shown in Fig. 1 A. In brief, the targeting vector comprised exons 6–9 of the *Cttn* gene, in which a neomycin cassette (flanked by Flp recombinase recognition sites) was inserted after exon 7 and two *loxP* sites were inserted flanking this exon. Targeted Cttn mut/WT ES (F1) cells were injected into C57BL/6J host blastocysts, which were then transferred into pseudopregnant females. Germline transmission of the targeted ES cells was confirmed by genotyping following standard procedures (DeChiara, 2001). The neomycin cassette was removed by crossing with mice expressing Flp recombinase (Rodríguez et al., 2000). Systemic Cre recombinase–mediated excision of exon 7 was achieved by crossing males carrying the floxed *Cttn* allele with transgenic females expressing Cre under the control of the human K14 promoter, allowing deletion in the oocyte (Hafner et al., 2004).

Genotyping. Genomic DNA was prepared from mouse tail samples as described previously (DeChiara, 2001). Genotyping for the WT, *Cttn*-targeted, and neomycin-containing deleted (del[neo]) alleles was described previously (Lai et al., 2009). Genotyping for the floxed (neo deleted) versus WT alleles was performed in a standard PCR setup using the following set of PCR primers: forward, fS, 5′-CTCTGCTCTGTGCTTTGACC-3′; and reverse, fA, 5′-GTGCTGTTCATCCACAATGC-3′, producing PCR fragments with a size of ∼150 bp (WT allele) and ∼370 bp (floxed allele). For the genotyping in Fig. 1 B, PCR primer sets forward, dS, (5′-AGGGTCTGAC-CATCATGTCC-3′) and reverse, fA (see above), were used, and PCR products generated were ∼400 bp for the deleted (KO) and ∼900 bp for the WT allele.

Intravital microscopy. 3 h before cremaster muscle exteriorization, *Cttn[del/del]* and sex- and age-matched *Cttn[WT/WT]* mice received 500 ng TNF (PeproTech) in 0.3 ml saline intrascrotally. Mice were anesthetized with an intraperitoneal injection of 125 mg/kg ketamine hydrochloride (Sanofi) and 12.5 mg/kg xylazine (TranquiVed; Phoenix Scientific), and the cremaster muscle was prepared for intravital microscopy as described previously (Zarbock et al., 2007, 2008). Postcapillary venules with a diameter between 20 and 40 μm were recorded using an intravital upright microscope (Axioskop; Carl Zeiss) with a 40× 0.75 saline immersion objective. Leukocyte rolling velocity, leukocyte rolling flux fraction, and leukocyte firm adhesion were determined by transillumination intravital microscopy. Leukocyte extravasation was investigated by reflected light oblique transillumination microscopy (Mempel et al., 2003; Mueller et al., 2010). Recorded images were analyzed using ImageJ (National Institutes of Health) and AxioVision (Carl Zeiss) software. The leukocyte rolling flux fraction was calculated as the percentage of total leukocyte flux. Emigrated cells were determined in an area reaching out 75 μm to each side of a vessel over a distance of 100 μm vessel length (representing 1.5×10^4 μm² tissue area). The microcirculation was recorded using a digital camera (Sensicam QE; PCO Inc.). Blood flow centerline velocity was measured using a dual photodiode sensor system (Circusoft Instrumentation). All animal experiments were approved by the Animal Care and Use Committees of the University of Münster and the local government. Animals were kept in a barrier facility under special pathogen-free conditions.

Bone marrow chimeras. Mixed chimeric mice were generated by performing bone marrow transplantation. In brief, bone marrow cells isolated from cortactin-deficient and WT littermate mice were separately injected i.v. into lethally irradiated WT mice (9.5 Gy). Experiments were performed 8 wk after bone marrow transplantation.

Determination of vascular permeability. Modified Miles assays were performed as described previously (Oura et al., 2003; Mamluk et al., 2005; Wegmann et al., 2006). In brief, three 8–12–wk-old *Cttn*^*del/del*^ and three sex- and age-matched *Cttn*^*WT/WT*^ mice were used per assay. Evans blue dye was injected into the tail vein, and 10 min later, 50 µl PBS or 100 ng histamine in 50 µl PBS was intradermally injected into the back skin that was shaved 24 h before the assay. 30 min later, animals were sacrificed, and skin areas surrounding the sites of injections were excised. Evans blue dye was extracted from the skin by incubation in formamide for 5 d at room temperature. Subsequently, the extracted dye was measured at 620 nm using a spectrophotometer. To exclude the possibility that the increase of Evans blue simply reflected the increase in blood flow, we measured the quantity of hemoglobin in the tissue by noninvasive white light spectroscopy using an O2C spectroscopy device (LEA Medizintechnik). The quantity of hemoglobin in the histamine-injected skin only increased by ∼20%. Thus, the increase of Evans blue detected in the histamine-stimulated skin was mainly caused by leakage and not by increased quantity of blood in the microvessel system.

Cell culture. HUVECs were isolated as described previously (Baumeister et al., 2005) and propagated in EGM endothelial cell growth medium (Lonza). ICAM-1^−/−^ endothelioma bendI1.1 and ICAM-1–retransfected bendI1.1 cells (provided by B. Engelhardt, University of Bern, Bern, Switzerland) were propagated as described previously (Lyck et al., 2003). The mouse endothelioma cell lines bend.3 and bend.5 cells were cultivated as described previously (Nottebaum et al., 2008). Human PMNs were isolated from the blood of healthy volunteers by Ficoll density gradient centrifugation as described previously (Moll et al., 1998). Murine bone marrow–derived leukocytes were isolated as described previously (Bixel et al., 2007). Primary MLECs were isolated from 8-wk-old *Cttn*^*del/del*^ and littermate *Cttn*^*WT/WT*^ mice as described previously (Schniedermann et al., 2010).

Transfections. siRNAs directed against the messenger RNAs of cortactin (QIAGEN) were transfected into HUVECs or mouse endothelioma cell lines by nucleofection (Lonza) as described previously (Nottebaum et al., 2008). Target sequences of oligonucleotides were as follows: human cortactin-5 (5′-CACCAGGAGCATATCAACATA-3′), human cortactin-6 (5′-ATGCAACTTATTGTATCTGAA-3′), murine cortactin-5 (5′-CAGAGATGTGCTAGTGGCTTA-3′), and murine cortactin-7 (5′-CACCAACATAGAAATGATTGA-3′). The AllStars Negative Control siRNA (no sequence provided; QIAGEN) served as nonsilencing negative control. Efficiency of knockdown was evaluated by Western blot or immunofluorescence staining of cortactin. Experiments were started 48 h after transfection. The two mouse and two human oligonucleotides each inhibited cortactin expression, permeability, and transmigration with similar efficiency. Experiments are shown with human cortactin-5 and mouse cortactin-5. The cDNA construct for CA and WT RhoG (Meller et al., 2008) was transfected into MLECs by nucleofection using the same conditions as for siRNA.

Western blotting. Equal protein amounts of cell lysates were separated by SDS-PAGE and transferred electrophoretically to polyvinylidenefluoride membranes (Millipore). After incubation in PBS containing 5% skim milk for 1 h to block unspecific binding, the membranes were probed in primary antibodies either for 4°C over night or for 1 h at 37°C, washed three times in PBS containing 0.5% skim milk and 0.05% Tween 20 for 10 min each, and incubated with species-specific peroxidase-conjugated secondary antibody (Dianova) for 1 h at 37°C. Chemiluminescence signals were recorded on Hyperfilm x-ray films (GE Healthcare). Tubulin blots were performed as loading controls.

Immunofluorescence microscopy. Cells were cultured as described in Cell culture, rinsed with PBS, and fixed in 100% ethanol at −20°C for 20 min. After washing, cells were incubated for 1 h in PBS containing 3% BSA to block unspecific binding. Coimmunolabeling with primary antibodies was performed for 1 h followed by washing and incubation with species-specific fluorescently labeled secondary antibodies (Invitrogen). Preparations were mounted in fluorescent mounting medium (Dako) and examined in a confocal laser-scanning microscope (Axiovert 200 M LSM510; Carl Zeiss).

For the determination of ICAM-1 clusters, adhesion of leukocytes to TNF-activated HUVECs was analyzed as described previously (Carman et al., 2003), except for that platelet-activating factor and MnCl₂ treatments were omitted. In brief, 500,000 PMNs were directly added to confluent HUVEC layers on a round 12-mm coverslip. After 20 min, cells were fixed in 4% paraformaldehyde and stained for microscopy.

Permeability assay. HUVECs or bend.3 endothelioma were nucleofected, seeded on 6.5-mm-diameter transwell filters (Corning) with 0.4-µm pore size, coated with 0.01% fibronectin, and cultured for 48 h before starting the assay. 4 × 10⁴ MLECs were seeded per 6.5-mm-diameter transwell filters with 3-µm pore size, coated with 0.01% fibronectin, and cultured for 1 wk before starting the assay. 0.25 mg/ml FITC-dextran (250 or 150 kD; Sigma Aldrich) was added to the top chamber, and diffusion was allowed for 30 min in the presence or absence of 100 µM 8-pCPT-2Me-cAMP at 37°C. Fluorescence in the lower chamber was measured using a spectrofluorimeter (Synergy-2; BioTek). Confluence of cells was determined by immunofluorescence staining for VE-cadherin for each assay. Transendothelial electrical resistance of HUVEC monolayers transfected and cultivated as described in Cell culture and Transfections was measured using a CellZScope device (nanoAnalytics) according to the manufacturer's instructions. The resistance of empty filters of 8.7 ± 0.6 Ω*cm² was subtracted from the values measured for the HUVEC monolayers.

Transmigration assay. PMN transmigration experiments with HUVEC and bend.5 monolayers, which were activated for 16 h with 5 nM TNF, were performed on 6.5-mm-diameter transwell filters with 5-µm pore size 48 h after transfection with siRNAs. 4 × 10⁴ MLECs were seeded per 6.5-mm-diameter transwell filters with 3-µm pore size, coated with 0.01% fibronectin, and cultured for 1 wk before starting the assay. In brief, cells were washed with 199 medium containing 20% FCS and 25 mM Hepes. The upper reservoir was then filled with 100 µl of supplemented 199 medium containing 0.5 × 10⁶ PMNs. After 1 h, the numbers of transmigrated PMNs in the lower reservoirs containing 500 µl of supplemented 199 medium were quantified using a Casy Cell Counter (Innovatis). PMN migration into the lower reservoirs is expressed as the percentage of total applied PMNs. Endothelial monolayers were controlled by immunofluorescence staining for VE-cadherin for each assay.

GTPase activity assays. To test for the activation levels of the small GTPase Rap1 in the absence of cortactin, GST-RalGDS-RBD pull-down experiments of Rap1-GTP were performed using the Rap1 Activation kit (Millipore) according to the manufacturer's instructions. Levels of active Rap1 were detected by Western blot using the antibody provided with the kit (Millipore). Western blots were scanned and quantified using ImageJ. To activate RhoG by ICAM-1 cross-linking, a 100-µl slurry of Dynabeads (Invitrogen) was loaded with 30 µg anti–ICAM-1 mAb YN1/1.7 (overnight) and added to a confluent monolayer of TNF-activated MLECs (7 × 10⁶ cells per 100-mm dish) for 30 min at 37°C. Unbound beads were washed off with ice-cold PBS before cell lysis. Aliquots of the cell lysates were snap frozen to determine later the total RhoG content. Active RhoG was precipitated from the remaining cell lysate using 50 µg ELMO-GST per sample (100-mm dish) as previously described (Meller et al., 2008). Levels of total and active RhoG were determined by Western blot using an anti-RhoG mAb provided by M.A. Schwartz.

Statistical analysis. Data are presented as mean with SD of the mean. Statistical significance was assessed using the Student's *t* test. χ² tests were performed for the mating statistics to test the probability that deviation between the observed and the expected values is caused by chance.

Online supplemental material. Fig. S1 shows that the expression of various endothelial surface receptors is not altered in the absence of cortactin. Fig. S2 shows that cortactin is undetectable in murine leukocytes and that systemic

cortactin deficiency does not cause alterations in leukocyte counts or in the expression level of various leukocyte surface receptors. Fig. S3 shows actin and VE-cadherin stainings of WT and KO MLECs. Fig. S4 shows cortactin knockdown effects in mouse endothelioma cells on Rap-1 activation, permeability, and neutrophil transmigration. Fig. S5 shows that cortactin deficiency enhances permeability of primary endothelial lung cell layers over time, which can be compensated by treatment with 007. Videos 1 and 2 show intravital microscopy of an inflamed cremaster muscle venule of a cortactin WT or cortactin KO animal, respectively. Tables S1 and S2 show mating statistics of heterozygous animals of mixed genetic background and from the sixth backcross to C57BL/6, respectively. Online supplemental material is available at http://www.jem.org/cgi/content/full/jem.20101920/DC1.

REFERENCES

Adamson, P., S. Etienne, P.O. Couraud, V. Calder, and J. Greenwood. 1999. Lymphocyte migration through brain endothelial cell monolayers involves signaling through endothelial ICAM-1 via a rho-dependent pathway. *J. Immunol*. 162:2964–2973.

Alcaide, P., S. Auerbach, and F.W. Luscinskas. 2009. Neutrophil recruitment under shear flow: it's all about endothelial cell rings and gaps. *Microcirculation*. 16:43–57. doi:10.1080/10739680802273892

Allingham, M.J., J.D. van Buul, and K. Burridge. 2007. ICAM-1–mediated, Src- and Pyk2-dependent vascular endothelial cadherin tyrosine phosphorylation is required for leukocyte transendothelial migration. *J. Immunol*. 179:4053–4064.

Ammer, A.G., and S.A. Weed. 2008. Cortactin branches out: roles in regulating protrusive actin dynamics. *Cell Motil. Cytoskeleton*. 65:687–707. doi:10.1002/cm.20296

Barreiro, O., M. Yanez-Mo, J.M. Serrador, M.C. Montoya, M. Vicente-Manzanares, R. Tejedor, H. Furthmayr, and F. Sanchez-Madrid. 2002. Dynamic interaction of VCAM-1 and ICAM-1 with moesin and ezrin in a novel endothelial docking structure for adherent leukocytes. *J. Cell Biol*. 157:1233–1245. doi:10.1083/jcb.200112126

Baumeister, U., R. Funke, K. Ebnet, H. Vorschmitt, S. Koch, and D. Vestweber. 2005. Association of Csk to VE-cadherin and inhibition of cell proliferation. *EMBO J*. 24:1686–1695. doi:10.1038/sj.emboj.7600647

Baumer, Y., D. Drenckhahn, and J. Waschke. 2008. cAMP induced Rac 1-mediated cytoskeletal reorganization in microvascular endothelium. *Histochem. Cell Biol*. 129:765–778. doi:10.1007/s00418-008-0422-y

Bixel, M.G., B. Petri, A.G. Khandoga, A. Khandoga, K. Wolburg-Buchholz, H. Wolburg, S. März, F. Krombach, and D. Vestweber. 2007. A CD99-related antigen on endothelial cells mediates neutrophil but not lymphocyte extravasation in vivo. *Blood*. 109:5327–5336. doi:10.1182/blood-2006-08-043109

Bixel, M.G., H. Li, B. Petri, A.G. Khandoga, A. Khandoga, A. Zarbock, K. Wolburg-Buchholz, H. Wolburg, L. Sorokin, D. Zeuschner, et al. 2010. CD99 and CD99L2 act at the same site as, but independently of, PECAM-1 during leukocyte diapedesis. *Blood*. 116:1172–1184. doi:10.1182/blood-2009-12-256388

Bosse, R., and D. Vestweber. 1994. Only simultaneous blocking of the L- and P-selectin completely inhibits neutrophil migration into mouse peritoneum. *Eur. J. Immunol*. 24:3019–3024. doi:10.1002/eji.1830241215

Burkhardt, J.K., E. Carrizosa, and M.H. Shaffer. 2008. The actin cytoskeleton in T cell activation. *Annu. Rev. Immunol*. 26:233–259. doi:10.1146/annurev.immunol.26.021607.090347

Carman, C.V., and T.A. Springer. 2004. A transmigratory cup in leukocyte diapedesis both through individual vascular endothelial cells and between them. *J. Cell Biol*. 167:377–388. doi:10.1083/jcb.200404129

Carman, C.V., C.D. Jun, A. Salas, and T.A. Springer. 2003. Endothelial cells proactively form microvilli-like membrane projections upon intercellular adhesion molecule 1 engagement of leukocyte LFA-1. *J. Immunol*. 171:6135–6144.

Cosen-Binker, L.I., and A. Kapus. 2006. Cortactin: the gray eminence of the cytoskeleton. *Physiology (Bethesda)*. 21:352–361.

Cullere, X., S.K. Shaw, L. Andersson, J. Hirahashi, F.W. Luscinskas, and T.N. Mayadas. 2005. Regulation of vascular endothelial barrier function by Epac, a cAMP-activated exchange factor for Rap GTPase. *Blood*. 105:1950–1955. doi:10.1182/blood-2004-05-1987

DeChiara, T.M. 2001. Gene targeting in ES cells. *Methods Mol. Biol*. 158:19–45.

Dudek, S.M., J.R. Jacobson, E.T. Chiang, K.G. Birukov, P. Wang, X. Zhan, and J.G. Garcia. 2004. Pulmonary endothelial cell barrier enhancement by sphingosine 1-phosphate: roles for cortactin and myosin light chain kinase. *J. Biol. Chem*. 279:24692–24700. doi:10.1074/jbc.M313969200

Dunne, J.L., C.M. Ballantyne, A.L. Beaudet, and K. Ley. 2002. Control of leukocyte rolling velocity in TNF-alpha-induced inflammation by LFA-1 and Mac-1. *Blood*. 99:336–341. doi:10.1182/blood.V99.1.336

Dunne, J.L., R.G. Collins, A.L. Beaudet, C.M. Ballantyne, and K. Ley. 2003. Mac-1, but not LFA-1, uses intercellular adhesion molecule-1 to mediate slow leukocyte rolling in TNF-alpha-induced inflammation. *J. Immunol*. 171:6105–6111.

Durieu-Trautmann, O., N. Chaverot, S. Cazaubon, A.D. Strosberg, and P.O. Couraud. 1994. Intercellular adhesion molecule 1 activation induces tyrosine phosphorylation of the cytoskeleton-associated protein cortactin in brain microvessel endothelial cells. *J. Biol. Chem*. 269:12536–12540.

Etienne-Manneville, S., J.B. Manneville, P. Adamson, B. Wilbourn, J. Greenwood, and P.O. Couraud. 2000. ICAM-1-coupled cytoskeletal rearrangements and transendothelial lymphocyte migration involve intracellular calcium signaling in brain endothelial cell lines. *J. Immunol*. 165:3375–3383.

Fukuhara, S., A. Sakurai, H. Sano, A. Yamagishi, S. Somekawa, N. Takakura, Y. Saito, K. Kangawa, and N. Mochizuki. 2005. Cyclic AMP potentiates vascular endothelial cadherin-mediated cell-cell contact to enhance endothelial barrier function through an Epac-Rap1 signaling pathway. *Mol. Cell. Biol*. 25:136–146. doi:10.1128/MCB.25.1.136-146.2005

Goley, E.D., and M.D. Welch. 2006. The ARP2/3 complex: an actin nucleator comes of age. *Nat. Rev. Mol. Cell Biol*. 7:713–726. doi:10.1038/nrm2026

Gotsch, U., E. Borges, R. Bosse, E. Böggemeyer, M. Simon, H. Mossmann, and D. Vestweber. 1997. VE-cadherin antibody accelerates neutrophil recruitment in vivo. *J. Cell Sci*. 110:583–588.

Hafner, M., J. Wenk, A. Nenci, M. Pasparakis, K. Scharffetter-Kochanek, N. Smyth, T. Peters, D. Kess, O. Holtkötter, P. Shephard, et al. 2004. Keratin 14 Cre transgenic mice authenticate keratin 14 as an oocyte-expressed protein. *Genesis*. 38:176–181. doi:10.1002/gene.20016

Hahne, M., M. Lenter, U. Jäger, S. Isenmann, and D. Vestweber. 1993. VCAM-1 is not involved in LPAM-1 (alpha 4 beta p/alpha 4 beta 7) mediated binding of lymphoma cells to high endothelial venules of mucosa-associated lymph nodes. *Eur. J. Cell Biol*. 61:290–298.

Hammel, M., G. Weitz-Schmidt, A. Krause, T. Moll, D. Vestweber, H.G. Zerwes, and R. Hallmann. 2001. Species-specific and conserved epitopes on mouse and human E-selectin important for leukocyte adhesion. *Exp. Cell Res*. 269:266–274. doi:10.1006/excr.2001.5317

Hidalgo, A., A.J. Peired, M.K. Wild, D. Vestweber, and P.S. Frenette. 2007. Complete identification of E-selectin ligands on neutrophils reveals distinct functions of PSGL-1, ESL-1, and CD44. *Immunity*. 26:477–489. doi:10.1016/j.immuni.2007.03.011

Jacobson, J.R., S.M. Dudek, P.A. Singleton, I.A. Kolosova, A.D. Verin, and J.G. Garcia. 2006. Endothelial cell barrier enhancement by ATP is

mediated by the small GTPase Rac and cortactin. *Am. J. Physiol. Lung Cell. Mol. Physiol.* 291:L289–L295. doi:10.1152/ajplung.00343.2005

Kai, M., M. Irie, T. Okutsu, K. Inoue, N. Ogonuki, H. Miki, M. Yokoyama, R. Migishima, K. Muguruma, H. Fujimura, et al. 2004. The novel dominant mutation Dspd leads to a severe spermiogenesis defect in mice. *Biol. Reprod.* 70:1213–1221. doi:10.1095/biolreprod.103.024802

Kansas, G.S., and F.M. Pavalko. 1996. The cytoplasmic domains of E- and P-selectin do not constitutively interact with alpha-actinin and are not essential for leukocyte adhesion. *J. Immunol.* 157:321–325.

Kanters, E., J. van Rijssel, P.J. Hensbergen, D. Hondius, F.P. Mul, A.M. Deelder, A. Sonnenberg, J.D. van Buul, and P.L. Hordijk. 2008. Filamin B mediates ICAM-1-driven leukocyte transendothelial migration. *J. Biol. Chem.* 283:31830–31839. doi:10.1074/jbc.M804888200

Khandoga, A., S. Huettinger, A.G. Khandoga, H. Li, S. Butz, K.W. Jauch, D. Vestweber, and F. Krombach. 2009. Leukocyte transmigration in inflamed liver: A role for endothelial cell-selective adhesion molecule. *J. Hepatol.* 50:755–765. doi:10.1016/j.jhep.2008.11.027

Kitamura, D., H. Kaneko, Y. Miyagoe, T. Ariyasu, and T. Watanabe. 1989. Isolation and characterization of a novel human gene expressed specifically in the cells of hematopoietic lineage. *Nucleic Acids Res.* 17: 9367–9379.

Kooistra, M.R., M. Corada, E. Dejana, and J.L. Bos. 2005. Epac1 regulates integrity of endothelial cell junctions through VE-cadherin. *FEBS Lett.* 579:4966–4972. doi:10.1016/j.febslet.2005.07.080

Kowalski, J.R., C. Egile, S. Gil, S.B. Snapper, R. Li, and S.M. Thomas. 2005. Cortactin regulates cell migration through activation of N-WASP. *J. Cell Sci.* 118:79–87. doi:10.1242/jcs.01586

Kumar, P., Q. Shen, C.D. Pivetti, E.S. Lee, M.H. Wu, and S.Y. Yuan. 2009. Molecular mechanisms of endothelial hyperpermeability: implications in inflammation. *Expert Rev. Mol. Med.* 11:e19. doi:10.1017/S1462399409001112

Kunkel, E.J., J.L. Dunne, and K. Ley. 2000. Leukocyte arrest during cytokine-dependent inflammation in vivo. *J. Immunol.* 164:3301–3308.

Lai, F.P., M. Szczodrak, J.M. Oelkers, M. Ladwein, F. Acconcia, S. Benesch, S. Auinger, J. Faix, J.V. Small, S. Polo, et al. 2009. Cortactin promotes migration and platelet-derived growth factor-induced actin reorganization by signaling to Rho-GTPases. *Mol. Biol. Cell.* 20:3209–3223. doi:10.1091/mbc.E08-12-1180

Ley, K., M. Allietta, D.C. Bullard, and S. Morgan. 1998. Importance of E-selectin for firm leukocyte adhesion in vivo. *Circ. Res.* 83:287–294.

Ley, K., C. Laudanna, M.I. Cybulsky, and S. Nourshargh. 2007. Getting to the site of inflammation: the leukocyte adhesion cascade updated. *Nat. Rev. Immunol.* 7:678–689. doi:10.1038/nri2156

Lyck, R., Y. Reiss, N. Gerwin, J. Greenwood, P. Adamson, and B. Engelhardt. 2003. T-cell interaction with ICAM-1/ICAM-2 double-deficient brain endothelium in vitro: the cytoplasmic tail of endothelial ICAM-1 is necessary for transendothelial migration of T cells. *Blood.* 102:3675–3683. doi:10.1182/blood-2003-02-0358

Mamluk, R., M. Klagsbrun, M. Detmar, and D.R. Bielenberg. 2005. Soluble neuropilin targeted to the skin inhibits vascular permeability. *Angiogenesis.* 8:217–227. doi:10.1007/s10456-005-9009-6

McEver, R.P. 2002. Selectins: lectins that initiate cell adhesion under flow. *Curr. Opin. Cell Biol.* 14:581–586. doi:10.1016/S0955-0674(02)00367-8

Meller, J., L. Vidali, and M.A. Schwartz. 2008. Endogenous RhoG is dispensable for integrin-mediated cell spreading but contributes to Rac-independent migration. *J. Cell Sci.* 121:1981–1989. doi:10.1242/jcs.025130

Mempel, T.R., C. Moser, J. Hutter, W.M. Kuebler, and F. Krombach. 2003. Visualization of leukocyte transendothelial and interstitial migration using reflected light oblique transillumination in intravital video microscopy. *J. Vasc. Res.* 40:435–441. doi:10.1159/000073902

Miner, J.J., L. Xia, T. Yago, J. Kappelmayer, Z. Liu, A.G. Klopocki, B. Shao, J.M. McDaniel, H. Setiadi, D.W. Schmidtke, and R.P. McEver. 2008. Separable requirements for cytoplasmic domain of PSGL-1 in leukocyte rolling and signaling under flow. *Blood.* 112:2035–2045. doi:10.1182/blood-2008-04-149468

Misra, A., R.P. Lim, Z. Wu, and T. Thanabalu. 2007. N-WASP plays a critical role in fibroblast adhesion and spreading. *Biochem. Biophys. Res. Commun.* 364:908–912. doi:10.1016/j.bbrc.2007.10.086

Moll, T., E. Dejana, and D. Vestweber. 1998. In vitro degradation of endothelial catenins by a neutrophil protease. *J. Cell Biol.* 140:403–407. doi:10.1083/jcb.140.2.403

Mueller, H., A. Stadtmann, H. Van Aken, E. Hirsch, D. Wang, K. Ley, and A. Zarbock. 2010. Tyrosine kinase Btk regulates E-selectin-mediated integrin activation and neutrophil recruitment by controlling phospholipase C (PLC) gamma2 and PI3Kgamma pathways. *Blood.* 115:3118–3127. doi:10.1182/blood-2009-11-254185

Nasdala, I., K. Wolburg-Buchholz, H. Wolburg, A. Kuhn, K. Ebnet, G. Brachtendorf, U. Samulowitz, B. Kuster, B. Engelhardt, D. Vestweber, and S. Butz. 2002. A transmembrane tight junction protein selectively expressed on endothelial cells and platelets. *J. Biol. Chem.* 277:16294–16303. doi:10.1074/jbc.M111999200

Nottebaum, A.F., G. Cagna, M. Winderlich, A.C. Gamp, R. Linnepe, C. Polaschegg, K. Filippova, R. Lyck, B. Engelhardt, O. Kamenyeva, et al. 2008. VE-PTP maintains the endothelial barrier via plakoglobin and becomes dissociated from VE-cadherin by leukocytes and by VEGF. *J. Exp. Med.* 205:2929–2945. doi:10.1084/jem.20080406

Ostermann, G., K.S. Weber, A. Zernecke, A. Schröder, and C. Weber. 2002. JAM-1 is a ligand of the beta(2) integrin LFA-1 involved in transendothelial migration of leukocytes. *Nat. Immunol.* 3:151–158. doi:10.1038/ni755

Oura, H., J. Bertoncini, P. Velasco, L.F. Brown, P. Carmeliet, and M. Detmar. 2003. A critical role of placental growth factor in the induction of inflammation and edema formation. *Blood.* 101:560–567. doi:10.1182/blood-2002-05-1516

Ren, G., M.S. Crampton, and A.S. Yap. 2009. Cortactin: Coordinating adhesion and the actin cytoskeleton at cellular protrusions. *Cell Motil. Cytoskeleton.* 66:865–873. doi:10.1002/cm.20380

Revenu, C., R. Athman, S. Robine, and D. Louvard. 2004. The co-workers of actin filaments: from cell structures to signals. *Nat. Rev. Mol. Cell Biol.* 5:635–646. doi:10.1038/nrm1437

Rodríguez, C.I., F. Buchholz, J. Galloway, R. Sequerra, J. Kasper, R. Ayala, A.F. Stewart, and S.M. Dymecki. 2000. High-efficiency deleter mice show that FLPe is an alternative to Cre-loxP. *Nat. Genet.* 25:139–140. doi:10.1038/75973

Schniedermann, J., M. Rennecke, K. Buttler, G. Richter, A.M. Städtler, S. Norgall, M. Badar, B. Barleon, T. May, J. Wilting, and H.A. Weich. 2010. Mouse lung contains endothelial progenitors with high capacity to form blood and lymphatic vessels. *BMC Cell Biol.* 11:50. doi:10.1186/1471-2121-11-50

Schnoor, M., and C.A. Parkos. 2008. Disassembly of endothelial and epithelial junctions during leukocyte transmigration. *Front. Biosci.* 13:6638–6652. doi:10.2741/3178

Selbach, M., and S. Backert. 2005. Cortactin: an Achilles' heel of the actin cytoskeleton targeted by pathogens. *Trends Microbiol.* 13:181–189. doi:10.1016/j.tim.2005.02.007

Setiadi, H., and R.P. McEver. 2008. Clustering endothelial E-selectin in clathrin-coated pits and lipid rafts enhances leukocyte adhesion under flow. *Blood.* 111:1989–1998. doi:10.1182/blood-2007-09-113423

Steeber, D.A., M.A. Campbell, A. Basit, K. Ley, and T.F. Tedder. 1998. Optimal selectin-mediated rolling of leukocytes during inflammation in vivo requires intercellular adhesion molecule-1 expression. *Proc. Natl. Acad. Sci. USA.* 95:7562–7567. doi:10.1073/pnas.95.13.7562

Takei, F. 1985. Inhibition of mixed lymphocyte response by a rat monoclonal antibody to a novel murine lymphocyte activation antigen (MALA-2). *J. Immunol.* 134:1403–1407.

Tanaka, S., M. Kunii, A. Harada, and S. Okabe. 2009. Generation of cortactin floxed mice and cellular analysis of motility in fibroblasts. *Genesis.* 47:638–646. doi:10.1002/dvg.20544

Thomas, S.G., S.D. Calaminus, J.M. Auger, S.P. Watson, and L.M. Machesky. 2007. Studies on the actin-binding protein HS1 in platelets. *BMC Cell Biol.* 8:46. doi:10.1186/1471-2121-8-46

Tilghman, R.W., and R.L. Hoover. 2002. The Src-cortactin pathway is required for clustering of E-selectin and ICAM-1 in endothelial cells. *FASEB J.* 16:1257–1259.

Turowski, P., R. Martinelli, R. Crawford, D. Wateridge, A.P. Papageorgiou, M.G. Lampugnani, A.C. Gamp, D. Vestweber, P. Adamson, E. Dejana, and J. Greenwood. 2008. Phosphorylation of vascular endothelial

cadherin controls lymphocyte emigration. *J. Cell Sci*. 121:29–37. doi:10.1242/jcs.022681

Uruno, T., P. Zhang, J. Liu, J.J. Hao, and X. Zhan. 2003. Haematopoietic lineage cell-specific protein 1 (HS1) promotes actin-related protein (Arp) 2/3 complex-mediated actin polymerization. *Biochem. J*. 371:485–493. doi:10.1042/BJ20021791

van Buul, J.D., and P.L. Hordijk. 2009. Endothelial adapter proteins in leukocyte transmigration. *Thromb. Haemost*. 101:649–655.

van Buul, J.D., M.J. Allingham, T. Samson, J. Meller, E. Boulter, R. García-Mata, and K. Burridge. 2007. RhoG regulates endothelial apical cup assembly downstream from ICAM1 engagement and is involved in leukocyte trans–endothelial migration. *J. Cell Biol*. 178:1279–1293. doi:10.1083/jcb.200612053

Vestweber, D. 2007. Adhesion and signaling molecules controlling the transmigration of leukocytes through endothelium. *Immunol. Rev*. 218:178–196. doi:10.1111/j.1600-065X.2007.00533.x

Vestweber, D., and J.E. Blanks. 1999. Mechanisms that regulate the function of the selectins and their ligands. *Physiol. Rev*. 79:181–213.

Vidal, C., B. Geny, J. Melle, M. Jandrot-Perrus, and M. Fontenay-Roupie. 2002. Cdc42/Rac1-dependent activation of the p21-activated kinase (PAK) regulates human platelet lamellipodia spreading: implication of the cortical-actin binding protein cortactin. *Blood*. 100:4462–4469. doi:10.1182/blood.V100.13.4462

Wang, H.B., J.T. Wang, L. Zhang, Z.H. Geng, W.L. Xu, T. Xu, Y. Huo, X. Zhu, E.F. Plow, M. Chen, and J.G. Geng. 2007. P-selectin primes leukocyte integrin activation during inflammation. *Nat. Immunol*. 8:882–892. doi:10.1038/ni1491

Weaver, A.M., J.E. Heuser, A.V. Karginov, W.L. Lee, J.T. Parsons, and J.A. Cooper. 2002. Interaction of cortactin and N-WASp with Arp2/3 complex. *Curr. Biol*. 12:1270–1278. doi:10.1016/S0960-9822(02)01035-7

Wegmann, F., B. Petri, A.G. Khandoga, C. Moser, A. Khandoga, S. Volkery, H. Li, I. Nasdala, O. Brandau, R. Fässler, et al. 2006. ESAM supports neutrophil extravasation, activation of Rho, and VEGF-induced vascular permeability. *J. Exp. Med*. 203:1671–1677. doi:10.1084/jem.20060565

Yang, L., J.R. Kowalski, P. Yacono, M. Bajmoczi, S.K. Shaw, R.M. Froio, D.E. Golan, S.M. Thomas, and F.W. Luscinskas. 2006a. Endothelial cell cortactin coordinates intercellular adhesion molecule-1 clustering and actin cytoskeleton remodeling during polymorphonuclear leukocyte adhesion and transmigration. *J. Immunol*. 177:6440–6449.

Yang, L., J.R. Kowalski, X. Zhan, S.M. Thomas, and F.W. Luscinskas. 2006b. Endothelial cell cortactin phosphorylation by Src contributes to polymorphonuclear leukocyte transmigration in vitro. *Circ. Res*. 98:394–402. doi:10.1161/01.RES.0000201958.59020.1a

Yoshida, M., W.F. Westlin, N. Wang, D.E. Ingber, A. Rosenzweig, N. Resnick, and M.A. Gimbrone Jr. 1996. Leukocyte adhesion to vascular endothelium induces E-selectin linkage to the actin cytoskeleton. *J. Cell Biol*. 133:445–455. doi:10.1083/jcb.133.2.445

Yu, D., H. Zhang, T.A. Blanpied, E. Smith, and X. Zhan. 2010. Cortactin is implicated in murine zygotic development. *Exp. Cell Res*. 316:848–858. doi:10.1016/j.yexcr.2009.11.018

Zarbock, A., and K. Ley. 2009. Neutrophil adhesion and activation under flow. *Microcirculation*. 16:31–42. doi:10.1080/10739680802350104

Zarbock, A., C.A. Lowell, and K. Ley. 2007. Spleen tyrosine kinase Syk is necessary for E-selectin-induced alpha(L)beta(2) integrin-mediated rolling on intercellular adhesion molecule-1. *Immunity*. 26:773–783. doi:10.1016/j.immuni.2007.04.011

Zarbock, A., C.L. Abram, M. Hundt, A. Altman, C.A. Lowell, and K. Ley. 2008. PSGL-1 engagement by E-selectin signals through Src kinase Fgr and ITAM adapters DAP12 and FcRγ to induce slow leukocyte rolling. *J. Exp. Med*. 205:2339–2347. doi:10.1084/jem.20072660

Zhan, X., C.C. Haudenschild, Y. Ni, E. Smith, and C. Huang. 1997. Upregulation of cortactin expression during the maturation of megakaryocytes. *Blood*. 89:457–464.